



Analysis of approximate solutions for neural signal propagation via the fractional Fitzhugh-Nagumo model

Hegagi Mohamed Ali*

Department of Mathematics, College of Science, University of Bisha, Bisha 61922, Saudi Arabia.
Department of Mathematics, Faculty of Science, Aswan University, Aswan 81528, Egypt.

Abstract

The Fitzhugh-Nagumo model (FNM) is essential for explaining how electrical signals travel through excitable material, such as nerve fibers, and how impulses are transmitted from the nerves. So, the key purpose of this article is to investigate a nonlinear transmission of the fractional order FNM using a computationally efficient analytical approach named the modified generalized Mittag-Leffler function method (MGMLFM). A more realistic formulation of the FNM with memory effects and non-local behavior has been obtained by generalizing it using the Caputo fractional operator. Furthermore, we study special cases derived from this fractional FNM that lead to other famous equations such as the fractional Newell-Whitehead model (NWM) and the fractional Zeldovich model (ZM). The MGMLFM approach to solving general fractional partial differential equations (FPDEs) is described. Additionally, the convergence and error analysis for this method are demonstrated. We illustrate the behavior of the approximate solution using graphical representations for varying values of the fractional operator α which converges to the exact solution when $\alpha = 1$. Additionally, the MGMLFM approximate values are contrasted with the known precise values in some tables which are exactly consistent with it when $\alpha = 1$, as well as, we compare the estimated absolute error from MGMLFM with other published methods under the same circumstances which is found to be much lower than comparable methods. The findings show the MGMLFM's effectiveness and advantages, which include its easily calculable components, direct implementation of the problems, satisfactory approximate solutions, small absolute error, and no need for linearization, perturbation, or transformations. So, the MGMLFM is a useful instrument for determining the outcomes of any more nonlinear problems that may arise in science and engineering.

Keywords. Fitzhugh-Nagumo model, Fractional partial differential equations, Mittag-Leffler function, Analytic approximate solutions.
2010 Mathematics Subject Classification. 35R11, 33E12, 35C10, 11Y35.

1. INTRODUCTION

The FNM is a nonlinear partial differential equation used to interpret many significant applications in applied mathematics, biology, physics, engineering and neuroscience areas such as the transmission of nerve impulses, circuit theory, the transmission of thermal energy in thermodynamics, and population genetics [15, 19, 27]. Since its first introduction by Fitzhugh [14], the classical form of FNM is presented as

$$\frac{\partial \mathcal{U}(x, t)}{\partial t} - \frac{\partial^2 \mathcal{U}(x, t)}{\partial x^2} - \mathcal{U}(x, t)(1 - \mathcal{U}(x, t))(\mathcal{U}(x, t) - \delta) = 0, \quad (1.1)$$

where $\mathcal{U}(x, t)$ indicates the transmembrane potential and δ is arbitrary constant. If $\delta = -1$, Eq. (1.1) transforms into the following classical NWM

$$\frac{\partial \mathcal{U}(x, t)}{\partial t} - \frac{\partial^2 \mathcal{U}(x, t)}{\partial x^2} - \mathcal{U}(x, t) + \mathcal{U}^3(x, t) = 0. \quad (1.2)$$

Received: 19 March 2025; Accepted: 05 January 2026.

* Corresponding author. Email: hegagi_math@aswu.edu.eg.

Also, when $\delta = 0$, Eq. (1.1) transforms into the following classical ZM

$$\frac{\partial \mathcal{U}(x, t)}{\partial t} - \frac{\partial^2 \mathcal{U}(x, t)}{\partial x^2} - \mathcal{U}^2(x, t) + \mathcal{U}^3(x, t) = 0. \quad (1.3)$$

The FNM has been extensively researched by many researchers [3, 8, 13, 30, 31].

In recent years, arbitrary order calculus or fractional calculus (FC) has been employed in many fields, including fluid dynamics, wave propagation equations, heat transfer, ocean circulation, etc. [1, 5, 23]. The FC is considered a generalization of integer order calculus [29]. The main goal of fractionalizing the order of differential equations is to leverage the feature of fractional-order derivatives to demonstrate memory effects. Where FC takes into account patrimonial aspects, system memory, and non-locality, all of which are essential for modeling real-world applications [4, 9]. The FC was developed with the help of world-renowned thinking mathematicians such as Euler, Fourier, Liouville, Lagrange, Riemann, Caputo and many others [20, 29]. However, the Caputo fractional derivative (CFD) is most widely used and significant among other fractional operators in representing many real-world applications because of its smoothness, satisfaction of the convolution theorem, and consistency with initial conditions. In addition, the CFD has favourable mathematical properties, such as linearity, compliance with initial conditions, and an intuitive physical dimension interpretation. Also, it offers a more intuitive and localized representation of fractional dynamics. Thus, it has a local character that makes it easier to understand and apply in a variety of scientific and engineering contexts. FC has recently become more popular and attracted the attention of many researchers because of its many uses in various science and engineering fields [2, 10].

Recently, partial differential equations (PDEs) have been used to model most physical phenomena and various applications in engineering and scientific areas [7, 16, 18, 21, 22, 24, 25, 28, 32]. The FPDEs are the name given to these PDEs with FC. Many researchers have been interested in FPDEs, and as a result, they have presented a variety of papers in that area and modeled complex real-life problems using nonlinear FPDEs [6, 11, 12]. The fractional order model (FOM) is characterized by the fact that it can be used at any stage and does not depend on the current state but on all historical states, in contrast to the integer-order models which depend only on the current state. It is also seen as a vital tool for predicting the future and describing the behavior of phenomena, and it is more effective in describing memory and hereditary properties than classical models. These are just a few of the important implications and advantages of using FOM.

Motivated by those aforementioned above, the objective of this work is to generalize the classical FNM Eq. (1.1) and its other special cases Eqs. (1.2) and (1.3) into time-fractional order. Furthermore, we discuss approximate solutions that are obtained in a reliable analytical method called MGMLFM. The mathematical framework of the suggested problems is provided as:

- the time-fractional FNM

$${}_0^C \mathcal{D}_t^\alpha \mathcal{U}(x, t) = \frac{\partial^2 \mathcal{U}(x, t)}{\partial x^2} + \mathcal{U}(x, t)(1 - \mathcal{U}(x, t))(\mathcal{U}(x, t) - \delta), \quad (1.4)$$

- the time-fractional NWM

$${}_0^C \mathcal{D}_t^\alpha \mathcal{U}(x, t) = \frac{\partial^2 \mathcal{U}(x, t)}{\partial x^2} + \mathcal{U}(x, t) - \mathcal{U}^3(x, t), \quad (1.5)$$

- the time-fractional ZM

$${}_0^C \mathcal{D}_t^\alpha \mathcal{U}(x, t) = \frac{\partial^2 \mathcal{U}(x, t)}{\partial x^2} + \mathcal{U}^2(x, t) - \mathcal{U}^3(x, t). \quad (1.6)$$

where ${}_0^C \mathcal{D}_t^\alpha$ is CFD with order $\alpha \in (0, 1]$, subject to initial condition

$$\mathcal{U}(x, 0) = \mathcal{U}_0(x). \quad (1.7)$$

This paper is innovative because it offers a trustworthy analytical technique, MGMLFM, for investigating the approximate solution of the time-fractional FNM Eq. (1.4) and its other special cases Eqs. (1.5) and (1.6) under appropriate initial condition Eq. (1.7). Moreover, we present in tabled data a comparison between the acquired approximate values at $\alpha = 1$ and recognized exact values, which demonstrate a complete agreement between the MGMLFM solution and the associated exact solution. To further elucidate the sufficiency and eligibility of MGMLFM,



we offer a comparison between the MGMLFM absolute error and other published methods under the same conditions published in [3, 13] such as conformable Sumudu decomposition method (CSDM), homotopy perturbation method (HPM), fourth residual power series (FRPS) and modified Taylor series technique (MTST), which turns out that the absolute error resulting from our method is much lower than that of comparable methods.

The remainder of this study is structured as follows. Essential preliminaries for FC are introduced in section 2, which helps us continue this research. Two subsections make up section 3: subsection 3.1 explains the general analysis of the suggested method, while subsection 3.2 proves the convergence theorem and discusses absolute error analysis. Section 4 is devoted to applying the proposed method to solve the time-fractional nonlinear FNM with appropriate initial conditions (ICs) at three different value of δ to give the previous cases presented in Eqs. (1.4), (1.5), and (1.6) which are explained in the subsections (4.1), (4.2), and (4.3), respectively. Additionally, we present a numerical simulation of the outcomes in figures with different fractional values, along with tables that allow comparisons between these solutions with the exact solutions and established techniques in these three subsections. The results of this study are concluded in section 5.

2. PRELIMINARIES

Some fundamental ideas and terminology are provided in this section to help further this study (see e.g. [9, 29]).

Definition 2.1. The definition of the Riemann-Liouville fractional integral is

$${}_0\mathcal{I}_t^\alpha \mathcal{F}(x, t) = \begin{cases} \frac{1}{\Gamma(\alpha)} \int_0^t (t - \zeta)^{\alpha-1} \mathcal{F}(x, \zeta) d\zeta, & \alpha > 0, \\ \mathcal{F}(x, t), & \alpha = 0. \end{cases}$$

Definition 2.2. For the absolutely continuous function $\mathcal{F}(x, t)$, the CFD is provided as

$${}_0^C\mathcal{D}_t^\alpha \mathcal{F}(x, t) = \begin{cases} \frac{1}{\Gamma(n-\alpha)} \int_0^t (t - \zeta)^{n-\alpha-1} \frac{\partial^n \mathcal{F}(x, \zeta)}{\partial \zeta^n} d\zeta, & \text{if } \alpha \in (n - 1, n]; n \in \mathbb{N}, \\ \frac{\partial^n \mathcal{F}(x, t)}{\partial t^n}, & \text{if } \alpha = n. \end{cases}$$

Theorem 2.3. Assuming $\mathcal{F}(x, t)$ is a differentiable function, then

$${}_0^C\mathcal{D}_t^\alpha {}_0\mathcal{I}_t^\alpha \mathcal{F}(x, t) = \mathcal{F}(x, t),$$

$${}_0\mathcal{I}_t^\alpha {}_0^C\mathcal{D}_t^\alpha \mathcal{F}(x, t) = \mathcal{F}(x, t) - \sum_{\kappa=0}^{n-1} \frac{\partial^\kappa \mathcal{F}(x, t)}{\partial t^\kappa} \Big|_{t=0} \frac{t^\kappa}{\kappa!}.$$

Definition 2.4. Suppose that the two-parameter Mittag-leffler function $\mathcal{M}(\cdot)$ is recognized by

$$\mathcal{M}_{\alpha, \beta}(t) = \sum_{\kappa=0}^{\infty} \frac{t^\kappa}{\Gamma(\kappa\alpha + \beta)}, \quad \alpha, \beta > 0, \tag{2.1}$$

when $\beta = 1$, the notation for it's $\mathcal{M}_\alpha(t)$.

Lemma 2.5. The CFD of $\mathcal{M}_\rho(\lambda t^\alpha)$ is specified by

$${}_0^C\mathcal{D}_t^\alpha \mathcal{M}_\alpha(\lambda t^\alpha) = \sum_{n=0}^{\infty} \frac{\lambda^{n+1} t^{n\alpha}}{\Gamma(n\alpha + 1)} = \lambda \mathcal{M}_\alpha(\lambda t^\alpha). \tag{2.2}$$

Theorem 2.6. [33] Let $\mathcal{N}(\cdot)$ is a nonlinear operator for the function $\mathcal{F}(\mathcal{X}, t) = \sum_{\kappa=0}^{\infty} \eta^\kappa \mathcal{F}_\kappa(\mathcal{X}, t)$, is supplied by

$$\mathcal{N}(\mathcal{F}) = \sum_{n=0}^{\infty} \left(\frac{1}{n!} \frac{\partial^n}{\partial \eta^n} \left[\mathcal{N} \left(\sum_{\kappa=0}^n \eta^\kappa \mathcal{F}_\kappa \right) \right]_{\eta=0} \right) \eta^n.$$

3. THEORETICAL ANALYSIS OF THE MGMLFM

There are two subsections in this section. The first offers a general solution for nonlinear FPDEs with the MGMLFM method. The investigation of absolute errors of the proposed method and the convergence theorem are discussed in the second part.



3.1. Analysis of MGMLFM. Here, we demonstrate the MGMLFM algorithm used to solve general nonlinear FPDEs.

$${}^C_0\mathcal{D}_t^\alpha \mathcal{F}(\mathfrak{X}, t) = \mathcal{L}(\mathcal{F}(\mathfrak{X}, t)) + \mathcal{N}(\mathcal{F}(\mathfrak{X}, t)), \quad (3.1)$$

with ICs

$$\mathcal{F}(\mathfrak{X}, 0) = \mathcal{H}(\mathfrak{X}), \quad (3.2)$$

where $\mathcal{F} = \begin{bmatrix} \mathcal{F}_1 \\ \mathcal{F}_2 \\ \vdots \\ \mathcal{F}_m \end{bmatrix}$, $\mathfrak{X} = [\mathfrak{x}_1 \ \mathfrak{x}_2 \ \dots \ \mathfrak{x}_n]$, $n, m \in \mathbb{N}$, $\mathcal{H}(\mathfrak{X}) = \begin{bmatrix} \mathcal{H}_1 \\ \mathcal{H}_2 \\ \vdots \\ \mathcal{H}_m \end{bmatrix}$, \mathcal{L} and \mathcal{N} are linear and nonlinear operators, respectively.

The MGMLFM imposes that the solution of Eq. (3.1) is given in the following form

$$\begin{aligned} \mathcal{F}_1(\mathfrak{X}, t) &= \mathcal{G}_1(\mathfrak{X}) \mathcal{M}_\alpha(\lambda_1 t^\alpha) = \sum_{k=0}^{\infty} \mathcal{G}_1(\mathfrak{X}) \lambda_1^k \frac{t^{k\alpha}}{\Gamma(k\alpha + 1)}, \\ \mathcal{F}_2(\mathfrak{X}, t) &= \mathcal{G}_2(\mathfrak{X}) \mathcal{M}_\alpha(\lambda_2 t^\alpha) = \sum_{k=0}^{\infty} \mathcal{G}_2(\mathfrak{X}) \lambda_2^k \frac{t^{k\alpha}}{\Gamma(k\alpha + 1)}, \\ &\vdots \\ \mathcal{F}_m(\mathfrak{X}, t) &= \mathcal{G}_m(\mathfrak{X}) \mathcal{M}_\alpha(\lambda_m t^\alpha) = \sum_{k=0}^{\infty} \mathcal{G}_m(\mathfrak{X}) \lambda_m^k \frac{t^{k\alpha}}{\Gamma(k\alpha + 1)}, \end{aligned} \quad (3.3)$$

where $\lambda_1, \dots, \lambda_m$ are unknown factors and $\mathcal{G}_1, \dots, \mathcal{G}_m$ are supportive functions satisfies $\mathcal{G}_1 = \mathcal{H}_1, \dots, \mathcal{G}_m = \mathcal{H}_m$. We can rewrite Eq. (3.1) as follows by applying Lemma 2.5 and Eq. (3.3).

$$\sum_{k=0}^{\infty} \mathcal{H}(\mathfrak{X}) \lambda_m^{k+1} \frac{t^{k\alpha}}{\Gamma(k\alpha + 1)} = \mathcal{L} \left(\sum_{k=0}^{\infty} \mathcal{H}(\mathfrak{X}) \lambda_m^k \frac{t^{k\alpha}}{\Gamma(k\alpha + 1)} \right) + \mathcal{N} \left(\sum_{k=0}^{\infty} \mathcal{H}(\mathfrak{X}) \lambda_m^k \frac{t^{k\alpha}}{\Gamma(k\alpha + 1)} \right). \quad (3.4)$$

Thus, the $\mathcal{L}(\cdot)$ is expressed as

$$\mathcal{L}(\mathcal{F}(\mathfrak{X}, t)) = \varpi \mathcal{H}(\mathfrak{X}) \sum_{k=0}^{\infty} \lambda_m^k \frac{t^{k\alpha}}{\Gamma(k\alpha + 1)}, \quad (3.5)$$

where ϖ is fixed. The $\mathcal{N}(\cdot)$ may be expressed using He's polynomials [17, 26] and Theorem 2.6 as follows

$$\mathcal{N}(\mathcal{F}(\mathfrak{X}, t)) = \mathcal{N}(\mathcal{H}(\mathfrak{X})) \left(\mathcal{N}(\mathcal{F}_0(\mathfrak{X}, t)) + \sum_{k=1}^{\infty} \left(\mathcal{N} \left(\sum_{i=0}^k \mathcal{F}_i(\mathfrak{X}, t) \right) - \mathcal{N} \left(\sum_{i=0}^{k-1} \mathcal{F}_i(\mathfrak{X}, t) \right) \right) \right). \quad (3.6)$$

Using Eqs. (3.5) and (3.6) into Eq. (3.4), we find a recurrence relation to get the coefficients λ_m . Then, the general solution of Eq. (3.1) is thus obtained.

3.2. Analysis of convergence and error. In this segment, we explain the convergence of the solution Eq. (3.1) and error analysis for the suggested method, while the solution's existence and uniqueness for the suggested model have been addressed in [8].

Theorem 3.1. *Let $\mathcal{F} = \mathcal{F}(\mathfrak{X}, t)$ is belongs to a Banach space \mathfrak{B} . Then, the series approximate solution specified in Eq. (3.1) is convergent if*

$$\|\mathcal{F}_{n+1}\| \leq \omega \|\mathcal{F}_n\|, \quad \forall \mathcal{F}_0 \in \mathfrak{B}; \quad n \in \mathbb{N},$$

where ω is a constant that satisfies $\omega \in (0, 1)$.

Proof. The proof of this theorem is the same manner in [8, 30]. □



Theorem 3.2. *If we have a constant $\omega \in (0, 1)$ such that $\|\mathcal{F}_{n+1}(\mathfrak{X}, t)\| \leq \omega \|\mathcal{F}_n(\mathfrak{X}, t)\|, \forall n \in \mathbb{N}$. Furthermore, if the truncated series $\sum_{n=0}^m \mathcal{F}_n(\mathfrak{X}, t)$ is regarded as an approximate solution of Eq. (3.1), then the maximum absolute error is presented as*

$$|\mathcal{F}(\mathfrak{X}, t) - \sum_{n=0}^m \mathcal{F}_n(\mathfrak{X}, t)| \leq \frac{\omega^{m+1}}{1 - \omega} \max_{(\mathfrak{X}, t) \in \omega} |\mathcal{F}_0(\mathfrak{X}, t)|.$$

Proof. Using Theorem 3.1, we have

$$\|\mathcal{S}_n - \mathcal{S}_m\| \leq \frac{\omega^{m+1}}{1 - \omega} \max_{(\mathfrak{X}, t) \in \omega} |\mathcal{F}_0(\mathfrak{X}, t)|.$$

Let $\mathcal{S}_n = \sum_{n=0}^m \mathcal{F}_n(\mathfrak{X}, t)$ for $m \rightarrow \infty$, then $\mathcal{S}_n \rightarrow \mathcal{F}(\mathfrak{X}, t)$, consequently

$$\|\mathcal{F}(\mathfrak{X}, t) - \mathcal{S}_m\| = \|\mathcal{F}(\mathfrak{X}, t) - \sum_{n=0}^m \mathcal{F}_n(\mathfrak{X}, t)\| \leq \frac{\omega^{m+1}}{1 - \omega} \max_{(\mathfrak{X}, t) \in \Omega} |\mathcal{F}_0(\mathfrak{X}, t)|.$$

Next, the maximum possible absolute truncation error is assessed as

$$|\mathcal{F}(\mathfrak{X}, t) - \sum_{n=0}^m \mathcal{F}_n(\mathfrak{X}, t)| \leq \frac{\omega^{m+1}}{1 - \omega} \max_{(\mathfrak{X}, t) \in \omega} |\mathcal{F}_0(\mathfrak{X}, t)|,$$

the theory is proven. □

4. APPLICATION AND RESULTS

4.1. Applying the described method to fractional FNM Eq. (1.4) when $\delta = -1$. In this part, we consider Eq. (1.4) when $\delta = -1$ (i.e, fractional NWM) [3], therefore the Eq. (1.4) is given as

$${}_0^C \mathcal{D}_t^\alpha \mathcal{U}(x, t) = \frac{\partial^2 \mathcal{U}(x, t)}{\partial x^2} + \mathcal{U}(x, t) - \mathcal{U}^3(x, t), \tag{4.1}$$

and the initial condition Eq. (1.7) is provided as

$$\mathcal{U}(x, 0) = \mathcal{U}_0(x) = \frac{1}{2}(1 + \tanh(\frac{\sqrt{2}x}{4})). \tag{4.2}$$

The exact solution of Eq. (4.1) when $\alpha = 1$ is specified as

$$\mathcal{U}(x, t) = \frac{1}{2}(1 + \tanh(\frac{\sqrt{2}x + 3t}{4})). \tag{4.3}$$

As per the MGMLFM procedures, the solution of Eq. (4.1) is presumed by

$$\mathcal{U}(x, t) = \mathcal{G}(x) \mathcal{M}_\alpha(\mathcal{A}t^\alpha) = \sum_{n=0}^\infty \mathcal{G}(x) \mathcal{A}^n \frac{t^{n\alpha}}{\Gamma(n\alpha + 1)}, \tag{4.4}$$

where $\mathcal{G}(x)$ is auxiliary function such that $\mathcal{G}(x) = \mathcal{U}_0(x)$ and \mathcal{A} is unknown factor. Utilizing Lemma 2.5 and Eq. (4.4), we have

$$\sum_{n=0}^\infty \left[\mathcal{U}_0 \mathcal{A}^{n+1} - \frac{\partial^2 (\mathcal{U}_0 \mathcal{A}^n)}{\partial x^2} - \mathcal{U}_0 \mathcal{A}^n + \mathcal{U}_0^3 C^n \Gamma(n\alpha + 1) \right] \frac{t^{n\alpha}}{\Gamma(n\alpha + 1)} = 0, \tag{4.5}$$

where

$$C^n = \sum_{k_1=0}^n \sum_{k_2=0}^{k_1} \frac{\mathcal{A}^{k_2} \mathcal{A}^{n-k_1} \mathcal{A}^{k_1-k_2}}{\Gamma(k_1\alpha + 1) \Gamma((n - k_1)\alpha + 1) \Gamma((k_1 - k_2)\alpha + 1)}. \tag{4.6}$$

From Eq. (4.5), the recurrence relation is presented as

$$\mathcal{A}^{n+1} = \frac{\frac{\partial^2 (\mathcal{U}_0 \mathcal{A}^n)}{\partial x^2} + \mathcal{U}_0 \mathcal{A}^n - \mathcal{U}_0^3 C^n \Gamma(n\alpha + 1)}{\mathcal{U}_0}. \tag{4.7}$$



By using Eq. (4.2), $\mathcal{A}^0 = 1$ and $n = 0, 1, 2, \dots$, we get

$$\mathcal{A}^1 = \frac{2(-\frac{1}{8}(\tanh(\frac{x}{2\sqrt{2}}) + 1)^3 + \frac{1}{2}(\tanh(\frac{x}{2\sqrt{2}}) + 1) - \frac{1}{8}\tanh(\frac{x}{2\sqrt{2}})\operatorname{sech}^2(\frac{x}{2\sqrt{2}}))}{\tanh(\frac{x}{2\sqrt{2}}) + 1}, \quad (4.8)$$

$$\begin{aligned} \mathcal{A}^2 = & -\frac{9(1 + 2\cosh(\sqrt{2}))\tanh(\frac{1}{\sqrt{2}})\operatorname{sech}^2(\frac{1}{\sqrt{2}})}{8(2\cosh(\sqrt{2}) - 1)^3(\tanh(\frac{3}{\sqrt{2}}) - 1)} - \frac{9\tanh(\sqrt{2})\operatorname{sech}^2(\sqrt{2})}{8 - 8\tanh(\sqrt{2})} - \frac{9\tanh(\frac{5}{\sqrt{2}})\operatorname{sech}^2(\frac{5}{\sqrt{2}})}{8(\tanh(\frac{5}{\sqrt{2}}) - 1)} \\ & - \frac{9\tanh(2\sqrt{2})\operatorname{sech}^2(2\sqrt{2})}{8(\tanh(2\sqrt{2}) - 1)} - \frac{9\tanh(2\sqrt{2})\operatorname{sech}^2(2\sqrt{2})}{8(1 + \tanh(2\sqrt{2}))} - \frac{9\tanh(\frac{5}{\sqrt{2}})\operatorname{sech}^2(\frac{5}{\sqrt{2}})}{8(1 + \tanh(\frac{5}{\sqrt{2}}))} \\ & - \frac{9(1 + 2\cosh(\sqrt{2}))\tanh(\frac{1}{\sqrt{2}})\operatorname{sech}^2(\frac{1}{\sqrt{2}})}{8(2\cosh(\sqrt{2}) - 1)^3(1 + \tanh(\frac{3}{\sqrt{2}}))}, \end{aligned} \quad (4.9)$$

$$\mathcal{A}^3 = \frac{27}{64}\operatorname{sech}^4(\frac{x}{2\sqrt{2}})\left(\frac{2(\cosh(\frac{x}{\sqrt{2}}) + \tanh(\frac{x}{2\sqrt{2}}) - 1)}{\tanh(\frac{x}{2\sqrt{2}}) + 1} - \frac{\Gamma(2\alpha + 1)}{\Gamma(\alpha + 1)^2}\right). \quad (4.10)$$

Thus, the remaining coefficients can be obtained by substituting different values of n . Therefore, the solution to Eq. (4.4) can be given in the form of the following power series:

$$\mathcal{U}(x, t) = \mathcal{U}_0(\mathcal{A}^0 + \mathcal{A}^1 \frac{t^\alpha}{\Gamma(\alpha + 1)} + \mathcal{A}^2 \frac{t^{2\alpha}}{\Gamma(2\alpha + 1)} + \mathcal{A}^3 \frac{t^{3\alpha}}{\Gamma(3\alpha + 1)} + \dots). \quad (4.11)$$

The following figures and tables offer the numerical simulation of these theoretical results. In Figure 1, we exhibit the behavior of approximate solution gained by MGMLFM at $\alpha = 1$ for \mathcal{U} in Eq. (4.1), and compare it with the exact solution in Eq. (4.3) through 2D and 3D to evaluate the accuracy and usefulness of the suggested method. We note that when $\alpha = 1$, the approximate solution is consistent with the exact solution. Also, as we increase x and t , we see that the solution behavior for \mathcal{U} increases. In Figure 2, we display the effect of different values of α on the behavior of the approximate solution in 2D and 3D plots. In 2D graphs, we keep $x = 8$ and show the behavior of \mathcal{U} with t , also, we set $t = 0.5$ and plot with x . We can observe that the solution of \mathcal{U} increases smoothly as the fractional values α decrease.

In Table 1, we present numerical values obtained by our method compared with numerical values of the exact solution as well as a comparison of the evaluated absolute errors for problem (4.1) between our technique and the CSDM published in [3] at different values of x when $\alpha = 1$, $t = 0.02$, and $t = 0.07$. In Table 2, we offer a comparison study of assessed absolute errors for \mathcal{U} between our method and MTST published in [13], at different values of x when $\alpha = 1$, $t = 0.1$ and $t = 0.5$. In Table 3, we provide another comparison study of assessed absolute errors for \mathcal{U} between current results and MTST published in [13], at different values of x when $\alpha = 1$, $t = 0.2$ and $t = 0.8$.

From the tabular results, it is clear that there is a high degree of agreement between the obtained solutions by MGMLFM and the exact solution presented. Furthermore, when compared to other previously published approaches, the absolute error calculated by MGMLFM is better and extremely minimal. We attest to the precision and effectiveness of the employed approach and suggest it as a useful tool for resolving further scientific applications represented by FPDEs in diverse scientific domains.

4.2. Applying the described method to fractional FNM Eq. (1.4) when $\delta = 0.75$. In this part, we consider Eq. (1.4) when $\delta = 0.75$ [3], therefore the Eq. (1.4) is given as

$${}_0^C \mathcal{D}_t^\alpha \mathcal{U}(x, t) = \frac{\partial^2 \mathcal{U}(x, t)}{\partial x^2} - \frac{3}{4}\mathcal{U}(x, t) + \frac{7}{4}\mathcal{U}^2(x, t) - \mathcal{U}^3(x, t), \quad (4.12)$$

and the initial condition Eq. (1.7) is provided as

$$\mathcal{U}(x, 0) = \mathcal{U}_0(x) = \frac{1}{1 + e^{-\left(\frac{x}{\sqrt{2}}\right)}}. \quad (4.13)$$



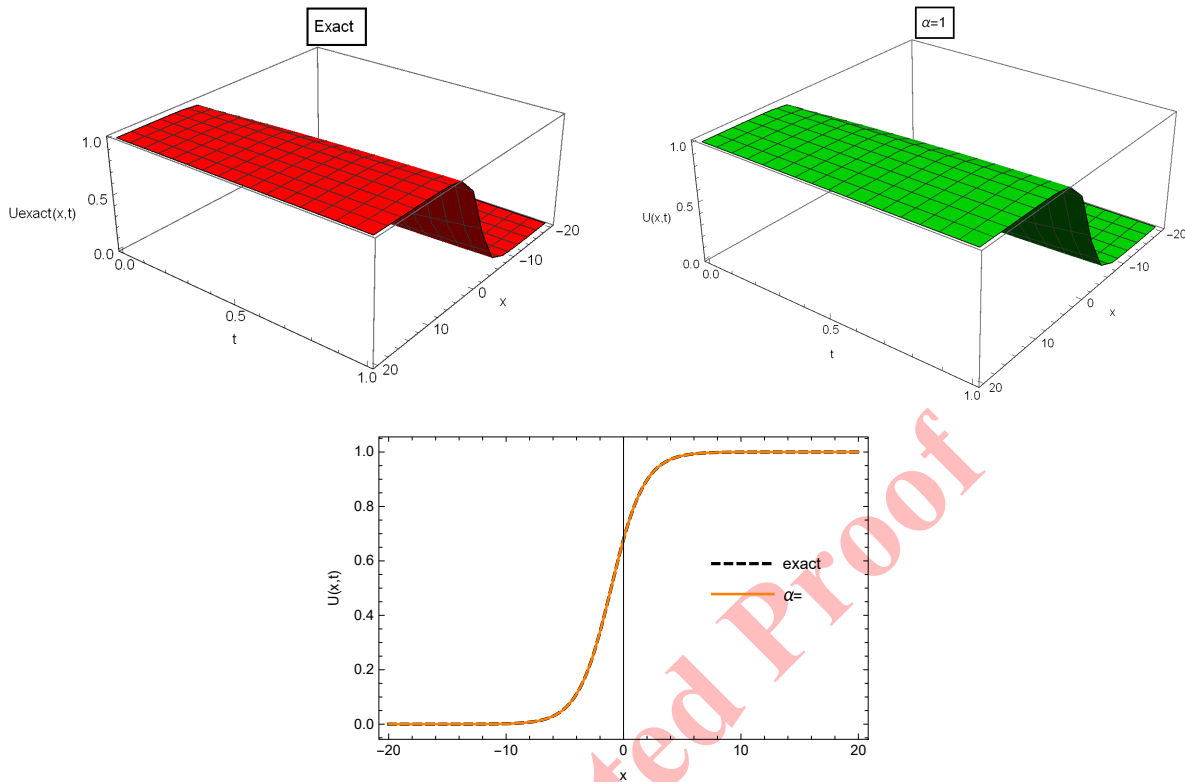


FIGURE 1. The behavior of the approximate solution in problem 4.1 when $\alpha = 1$ and exact solution for $\mathcal{U}(x, t)$ in three and two dimensions.

TABLE 1. The exact solution, the approximate solution of MGMLFM (current results) for problem 4.1 and a comparison of the absolute error with CSDM [3] at distinct values of x when $\alpha = 1$, $t = 0.02$ and $t = 0.07$.

x	$t = 0.02$				$t = 0.07$			
	Exact	MGMLFM	CSDM error	MGMLFM Error	Exact	MGMLFM	CSDM error	MGMLFM Error
0.05	0.516333	0.516333	1.11929×10^{-6}	3.48495×10^{-10}	0.535031	0.535031	4.75469×10^{-5}	7.1145×10^{-8}
0.10	0.525156	0.525156	1.11497×10^{-6}	6.44521×10^{-10}	0.543815	0.543815	4.73493×10^{-5}	1.15354×10^{-7}
0.15	0.533964	0.533964	1.10789×10^{-6}	9.37136×10^{-10}	0.552571	0.552571	4.70361×10^{-5}	1.58953×10^{-7}
0.20	0.542751	0.542751	1.09809×10^{-6}	1.22481×10^{-9}	0.561295	0.561295	4.66091×10^{-5}	2.01715×10^{-7}
0.25	0.551511	0.551511	1.08563×10^{-6}	1.50605×10^{-9}	0.569982	0.569982	4.60706×10^{-5}	2.43422×10^{-7}

The exact solution of Eq. (4.12) when $\alpha = 1$ is specified as

$$\mathcal{U}(x, t) = \frac{1}{1 + e^{-\frac{1}{\sqrt{2}}(x + \frac{t}{2})}}. \tag{4.14}$$

In the same manner as in the analysis of problem (4.1), the recurrence relation of Eq. (4.12) given as

$$\mathcal{A}^{n+1} = \frac{\frac{\partial^2 (\mathcal{U}_0 \mathcal{A}^n)}{\partial x^2} - \frac{3}{4} \mathcal{U}_0 \mathcal{A}^n + \frac{7}{4} \mathcal{U}_0^2 L^n \Gamma(n\alpha + 1) - \mathcal{U}_0^3 C^n \Gamma(n\alpha + 1)}{\mathcal{U}_0}, \tag{4.15}$$



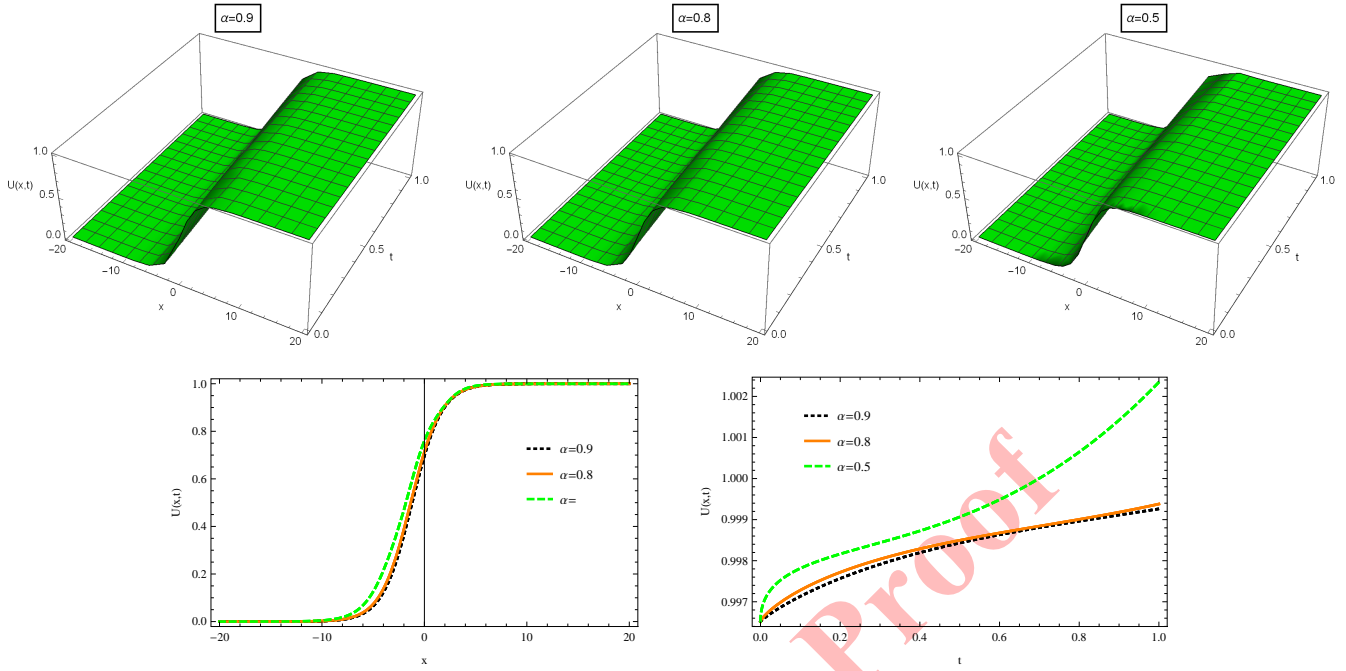


FIGURE 2. The behavior of approximate solution for $\mathcal{U}(x, t)$ problem 4.1 at $\alpha = 0.9, 0.8, 0.5$ in three dimensions as well as two dimensions with x at $t = 0.5$ and with t at $x = 8$.

TABLE 2. The exact solution, the approximate solution of MGMLFM (current results) for problem 4.1 and a comparison of the absolute error with MTST [13] at distinct values of x when $\alpha = 1, t = 0.1$ and $t = 0.5$.

x	$t = 0.1$				$t = 0.5$			
	Exact	MGMLFM	MGMLFM Error	MTST Error	Exact	MGMLFM	MGMLFM Error	MTST Error
-10	0.000985	0.000985803	1.29747×10^{-11}	1.81907×10^{-8}	0.001794	0.00179457	2.20492×10^{-7}	1.28995×10^{-5}
-8	0.004042	0.00404245	4.40827×10^{-11}	7.04021×10^{-8}	0.007341	0.00734069	7.32639×10^{-7}	5.03538×10^{-5}
-6	0.016420	0.0164209	4.76152×10^{-11}	1.61065×10^{-7}	0.029522	0.0295218	5.50836×10^{-7}	1.62080×10^{-4}
-4	0.064258	0.0642584	8.91485×10^{-10}	4.24470×10^{-6}	0.111211	0.111227	1.59214×10^{-5}	3.41467×10^{-5}
6	0.987783	0.987783	5.18448×10^{-11}	3.02488×10^{-4}	0.993258	0.993259	8.98414×10^{-7}	7.67840×10^{-3}
8	0.997002	0.997002	4.27119×10^{-11}	7.73833×10^{-5}	0.998353	0.998353	6.26366×10^{-7}	1.97000×10^{-3}
10	0.999270	0.99927	1.24604×10^{-11}	1.90502×10^{-5}	0.999599	0.999599	1.80122×10^{-7}	4.85362×10^{-4}

TABLE 3. The exact solution, the approximate solution of MGMLFM (current results) for problem 4.1 and a comparison of the absolute error with HPM [13] at distinct values of x when $\alpha = 1, t = 0.2$ and $t = 0.8$.

x	$t = 0.2$				$t = 0.8$			
	Exact	MGMLFM	MGMLFM Error	HPM Error	Exact	MGMLFM	MGMLFM Error	HPM Error
-10	0.001145	0.00114516	8.47669×10^{-10}	4.09642×10^{-6}	0.002811	0.00280798	3.95024×10^{-6}	3.36424×10^{-4}
-8	0.004693	0.00469358	2.86584×10^{-9}	1.64667×10^{-5}	0.011465	0.011453	1.28387×10^{-5}	1.34099×10^{-3}
-6	0.019027	0.0190278	2.88383×10^{-9}	6.15644×10^{-5}	0.045536	0.0455306	5.627×10^{-6}	4.84162×10^{-3}
-4	0.073889	0.0738893	5.9072×10^{-8}	1.67637×10^{-4}	0.164046	0.164337	2.91138×10^{-4}	1.13031×10^{-2}
6	0.989467	0.989467	3.4287×10^{-9}	5.39335×10^{-5}	0.995691	0.995706	157108×10^{-5}	2.86839×10^{-3}
8	0.997419	0.997419	2.69056×10^{-9}	1.42325×10^{-5}	0.998949	0.998959	1.00245×10^{-5}	7.47603×10^{-4}
10	0.999371	0.999371	7.81804×10^{-10}	3.52926×10^{-6}	0.999744	0.999747	2.85821×10^{-6}	1.84838×10^{-4}



where

$$L^n = \sum_{k=0}^n \frac{\mathcal{A}^k \mathcal{A}^{(n-k)}}{\Gamma(k\alpha + 1)\Gamma((n-k)\alpha + 1)}, \tag{4.16}$$

and C^n as presented in Eq. (4.6). Using Eq. (4.13), $\mathcal{A}^0 = 1$ and $n = 0, 1, 2, \dots$, we have

$$\mathcal{A}^1 = (e^{-\frac{x}{\sqrt{2}} + 1}) \left(\frac{1.75}{(e^{-\frac{x}{\sqrt{2}} + 1})^2} - \frac{e^{-\frac{x}{\sqrt{2}}}}{2(e^{-\frac{x}{\sqrt{2}} + 1})^2} + \frac{e^{-\sqrt{2}x}}{(e^{-\frac{x}{\sqrt{2}} + 1})^3} - \frac{1}{(e^{-\frac{x}{\sqrt{2}} + 1})^3} - \frac{0.75}{e^{-\frac{x}{\sqrt{2}} + 1}} \right), \tag{4.17}$$

$$\mathcal{A}^2 = \frac{0.0625 + 0.0625e^{\frac{x}{\sqrt{2}}} - 0.0625e^{\frac{3x}{\sqrt{2}}} - 0.0625e^{\sqrt{2}x}}{(1. + e^{\frac{x}{\sqrt{2}}})^4}, \tag{4.18}$$

$$\mathcal{A}^3 = \frac{\psi}{(1. + e^{\frac{x}{\sqrt{2}}})^6 \Gamma(\alpha + 1)^2}, \tag{4.19}$$

where

$$\begin{aligned} \psi = & (-0.203125e^{\frac{x}{\sqrt{2}}} + 0.21875e^{\frac{3x}{\sqrt{2}}} - 0.015625e^{\frac{5x}{\sqrt{2}}} - 0.15625e^{\sqrt{2}x} + 0.171875e^{2\sqrt{2}x} - 0.015625)\Gamma(\alpha + 1)^2 \\ & - 0.078125e^{\frac{x}{\sqrt{2}}} \left(1.e^{\frac{x}{\sqrt{2}}} - 1.4\right) \left(1. + 1.e^{\frac{x}{\sqrt{2}}}\right)^2 \Gamma(2\alpha + 1). \end{aligned}$$

We can find other coefficients in the same way, and substituted into the following power series to obtain the approximate solution:

$$\mathcal{U}(x, t) = \mathcal{U}_0(\mathcal{A}^0 + \mathcal{A}^1 \frac{t^\alpha}{\Gamma(\alpha + 1)} + \mathcal{A}^2 \frac{t^{2\alpha}}{\Gamma(2\alpha + 1)} + \mathcal{A}^3 \frac{t^{3\alpha}}{\Gamma(3\alpha + 1)} + \dots). \tag{4.20}$$

The numerical simulation of this case is presented in the next figures and tables. In Figure 3, we compare the solution of \mathcal{U} in Eq. (4.12) gained by MGMLFM at $\alpha = 1$ with the known exact solution given in Eq. (4.14) through 2D and 3D in order to present the accuracy and efficiency of MGMLFM. We observe that when $\alpha = 1$, the approximate solution converges to the exact solution. Also, by increasing x and t , the behavior solution of \mathcal{U} increases. In Figure 4, we show the impact of various values of α on the behavior of the approximate solution in 2D and 3D plots. In 2D graphs, we keep $x = 0.5$ and show the behavior of \mathcal{U} with t , also, we set $t = 0.05$ and plot with x . We observe that in the case of plotting with x , the solutions are close for different α values. On the contrary, the difference is very clear between the solutions when plotting with t for different α values. In both cases, we notice that the behavior of the solution increases smoothly with the decrease in the fractional α values.

In Table 4, we offer numerical values obtained by MGMLFM compared with numerical values of the exact solution as well as a comparison of the evaluated absolute errors for the problem (4.12) between our method and the CSDM published in [3] at different values of x when $\alpha = 1$, $t = 0.01$, and $t = 0.05$. The tabular data clearly shows that the approximate solutions produced by MGMLFM and the exact solution that is displayed have a high degree of agreement. Additionally, when compared to other previously published approaches, the absolute error calculated by MGMLFM is extremely minimal, which demonstrates the accuracy and effectiveness of our method in solving FPDEs compared to others.

4.3. Applying the described method to fractional FNM Eq. (1.4) when $\delta = 0$. Here, we consider Eq. (1.4) when $\delta = 0$ (i.e., fractional ZM) [3], consequently it's identified as

$${}^C_0D_t^\alpha \mathcal{U}(x, t) = \frac{\partial^2 \mathcal{U}(x, t)}{\partial x^2} + \mathcal{U}^2(x, t) - \mathcal{U}^3(x, t), \tag{4.21}$$

and the initial condition Eq. (1.7) is provided as

$$\mathcal{U}(x, 0) = \mathcal{U}_0(x) = \frac{1}{2} + \frac{1}{2} \tanh\left(\frac{\sqrt{2}x}{4}\right). \tag{4.22}$$



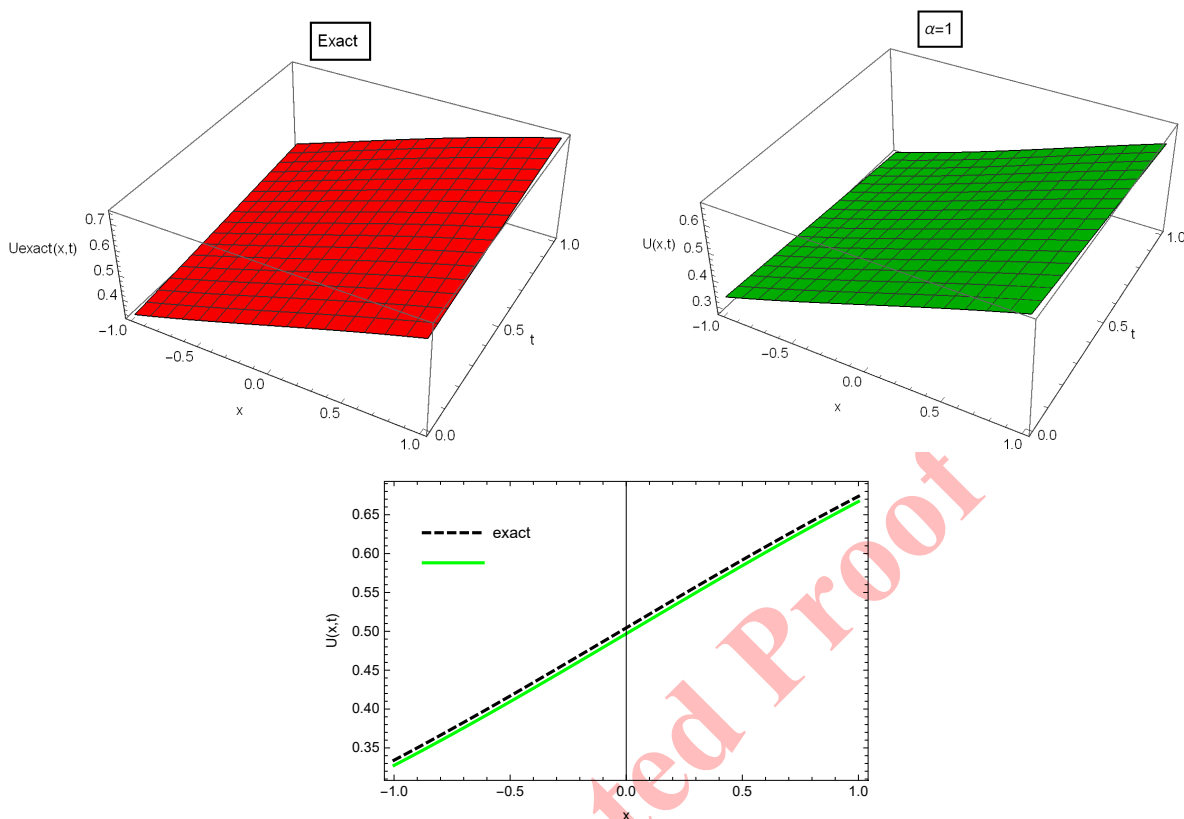


FIGURE 3. The behavior of approximate solution in problem 4.2 when $\alpha = 1$ and exact solution for $\mathcal{U}(x, t)$ in three and two dimensions.

TABLE 4. The exact solution, the approximate solution of MGMLFM (current results) for problem 4.2 and a comparison of the absolute error with CSDM [3] at distinct values of x when $\alpha = 1$, $t = 0.01$ and $t = 0.05$.

x	$t = 0.01$				$t = 0.05$			
	Exact	MGMLFM	CSDM error	MGMLFM Error	Exact	MGMLFM	CSDM error	MGMLFM Error
0.05	0.509721	0.508213	7.48392×10^{-3}	1.5084×10^{-3}	0.513255	0.505714	7.48392×10^{-3}	7.54156×10^{-3}
0.10	0.518553	0.517046	7.5053×10^{-3}	1.50697×10^{-3}	0.522083	0.514549	7.5053×10^{-3}	7.53415×10^{-3}
0.15	0.527373	0.525868	7.52205×10^{-3}	1.50461×10^{-3}	0.530897	0.523374	7.52205×10^{-3}	7.52205×10^{-3}
0.20	0.536176	0.534675	7.53415×10^{-3}	1.50131×10^{-3}	0.539691	0.532186	7.53415×10^{-3}	7.5053×10^{-3}
0.25	0.544956	0.543459	7.54156×10^{-3}	1.49709×10^{-3}	0.548461	0.540977	7.54156×10^{-3}	7.48392×10^{-3}

The exact solution of Eq. (4.21) when $\alpha = 1$ is specified as

$$\mathcal{U}(x, t) = \frac{1}{2} \left(1 + \tanh\left(\frac{\sqrt{2}x + t}{4}\right) \right). \quad (4.23)$$

Similar to how the problems analysis (4.1) and (4.2) were conducted, the recurrence relation of Eq. (4.21) is provided as

$$\mathcal{A}^{n+1} = \frac{\frac{\partial^2(\mathcal{U}_0 \mathcal{A}^n)}{\partial x^2} + \mathcal{U}_0^2 L^n \Gamma(n\alpha + 1) - \mathcal{U}_0^3 C^n \Gamma(n\alpha + 1)}{\mathcal{U}_0}, \quad (4.24)$$



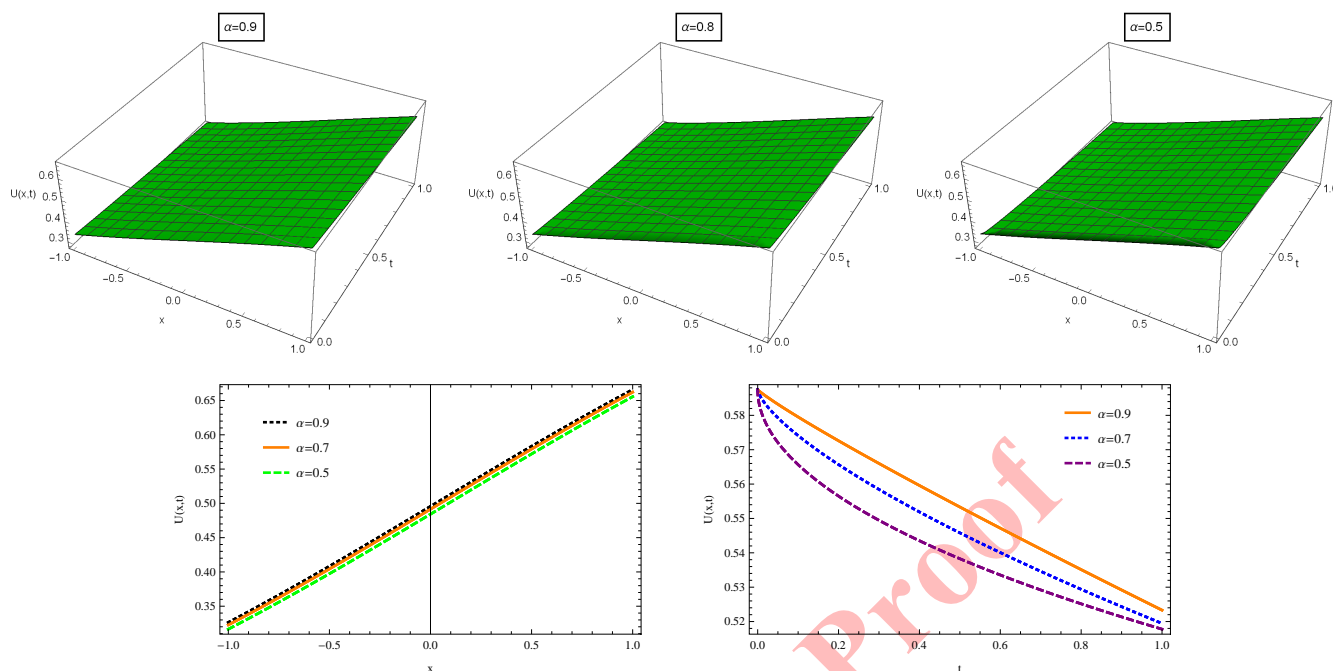


FIGURE 4. The behavior of approximate solution for $\mathcal{U}(x, t)$ problem 4.2 at $\alpha = 0.9, 0.8, 0.5$ in three dimensions as well as two dimensions with x at $t = 0.05$ and with t at $x = 0.5$.

where L^n as Eq. (4.16) and C^n as Eq. (4.6). Using Eq. (4.22), $\mathcal{A}^0 = 1$ and $n = 0, 1, 2, \dots$, we have

$$\mathcal{A}^1 = \frac{2(-\frac{1}{8}(\tanh(\frac{x}{2\sqrt{2}}) + 1)^3 + \frac{1}{4}(\tanh(\frac{x}{2\sqrt{2}}) + 1)^2 - \frac{1}{8}\tanh(\frac{x}{2\sqrt{2}})\text{sech}^2(\frac{x}{2\sqrt{2}}))}{\tanh(\frac{x}{2\sqrt{2}}) + 1}, \tag{4.25}$$

$$\mathcal{A}^2 = -\frac{\sinh^4(\frac{x}{2\sqrt{2}})\text{csch}^3(\frac{x}{\sqrt{2}})}{\tanh(\frac{x}{2\sqrt{2}}) + 1}, \tag{4.26}$$

$$\mathcal{A}^3 = \frac{\text{sech}^4(\frac{x}{2\sqrt{2}})(2\Gamma(\alpha + 1)^2(\cosh(\frac{x}{\sqrt{2}}) + 3\tanh(\frac{x}{2\sqrt{2}}) - 1) - \Gamma(2\alpha + 1)(3\tanh(\frac{x}{2\sqrt{2}}) + 1))}{64\Gamma(\alpha + 1)^2(\tanh(\frac{x}{2\sqrt{2}}) + 1)}. \tag{4.27}$$

To get the approximate solution, we can obtain further coefficients in the same manner and substitute them into the power series that follows:

$$\mathcal{U}(x, t) = \mathcal{U}_0(\mathcal{A}^0 + \mathcal{A}^1 \frac{t^\alpha}{\Gamma(\alpha + 1)} + \mathcal{A}^2 \frac{t^{2\alpha}}{\Gamma(2\alpha + 1)} + \mathcal{A}^3 \frac{t^{3\alpha}}{\Gamma(3\alpha + 1)} + \dots). \tag{4.28}$$

The simulation of these results is presented in the following plots and tables. In Figure 5, we compare the exact solution in Eq. (4.23) in 2D and 3D with the behavior of the obtained solution by MGMLFM at $\alpha = 1$ for \mathcal{U} in Eq. (4.21), to assess the precision and utility of the proposed approach. We observe that the approximate solution and the exact solution are consistent when $\alpha = 1$. Additionally, we observe that the solution behavior for \mathcal{U} grows when we raise x and t . We show how different choices of α affect the behavior of the approximation solution in 2D and 3D plots in Figure 6. In 2D graphs, we set $t = 0.5$ and plot with x , and we maintain $x = 5$ to demonstrate the behavior of \mathcal{U} with t . As the fractional values α drop, we can see that the solution of \mathcal{U} grows gradually.

In Table 5, we provide the numerical values acquired by our method for problem 4.3 along with numerical values of the exact solution Eq. (4.23). Also, a comparison for evaluated absolute errors between MGMLFM with FRPS



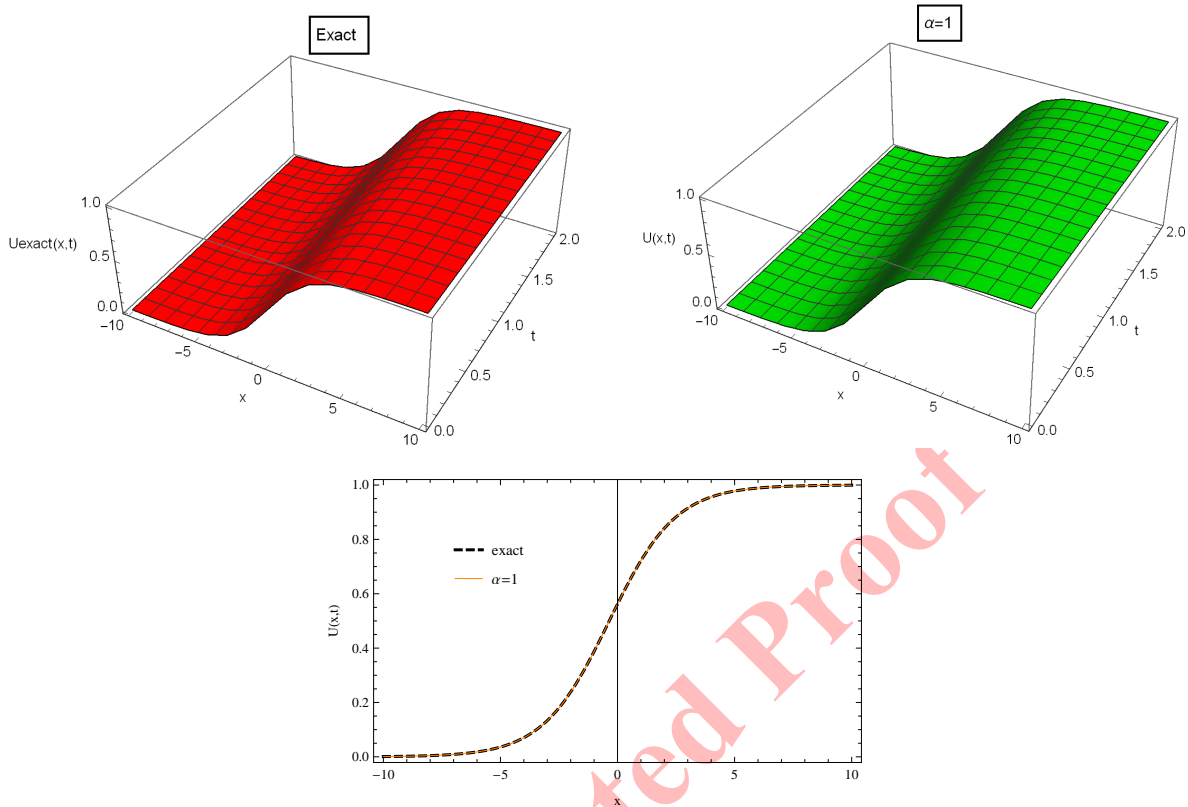


FIGURE 5. The behavior of approximate solution in problem 4.3 when $\alpha = 1$ and exact solution for $\mathcal{U}(x, t)$ in three and two dimensions.

TABLE 5. The exact solution, the approximate solution of MGMLFM (current results) for problem 4.3 and a comparison of the absolute error with FRPS [13] at distinct values of x when $\alpha = 1$, $t = 0.5$ and $t = 1.5$.

x	$t = 0.5$				$t = 1.5$			
	Exact	MGMLFM	MGMLFM Error	FRPS Error	Exact	MGMLFM	MGMLFM Error	FRPS Error
-8	0.004465	0.0044657	9.54777×10^{-10}	3.47646×10^{-10}	0.007341	0.00734069	7.32639×10^{-7}	1.09671×10^{-8}
-6	0.0181167	0.0181167	9.84808×10^{-10}	2.12363×10^{-8}	0.029522	0.0295218	5.50836×10^{-7}	6.31389×10^{-7}
-4	0.0705398	0.0705398	1.95568×10^{-8}	8.71566×10^{-7}	0.111210	0.111227	1.59214×10^{-5}	2.09979×10^{-5}
4	0.955994	0.955994	1.73759×10^{-8}	1.47459×10^{-5}	0.972839	0.972828	1.12293×10^{-5}	3.55260×10^{-4}
6	0.988933	0.988933	1.13647×10^{-9}	1.47787×10^{-6}	0.993258	0.993259	8.98414×10^{-7}	4.39392×10^{-5}
8	0.997287	0.997287	9.05841×10^{-10}	9.95126×10^{-8}	0.998353	0.998353	6.26366×10^{-7}	3.13930×10^{-6}
10	0.999339	0.999339	2.63554×10^{-10}	6.07206×10^{-9}	0.999599	0.999599	1.80122×10^{-7}	1.94396×10^{-7}

method published in [13] at various values of x when $\alpha = 1$, $t = 0.5$, and $t = 1.5$. We provide a another comparison study of assessed absolute errors for \mathcal{U} between our method and MTST technique published in [13], at different values of x for $\alpha = 1$, $t = 0.1$, and $t = 0.5$, in Table 6. Moreover, another comparison study of assessed absolute errors for \mathcal{U} between current results and HPM reported in [13] is presented in Table 7, at various values of x when $\alpha = 1$, $t = 0.2$, and $t = 0.8$.



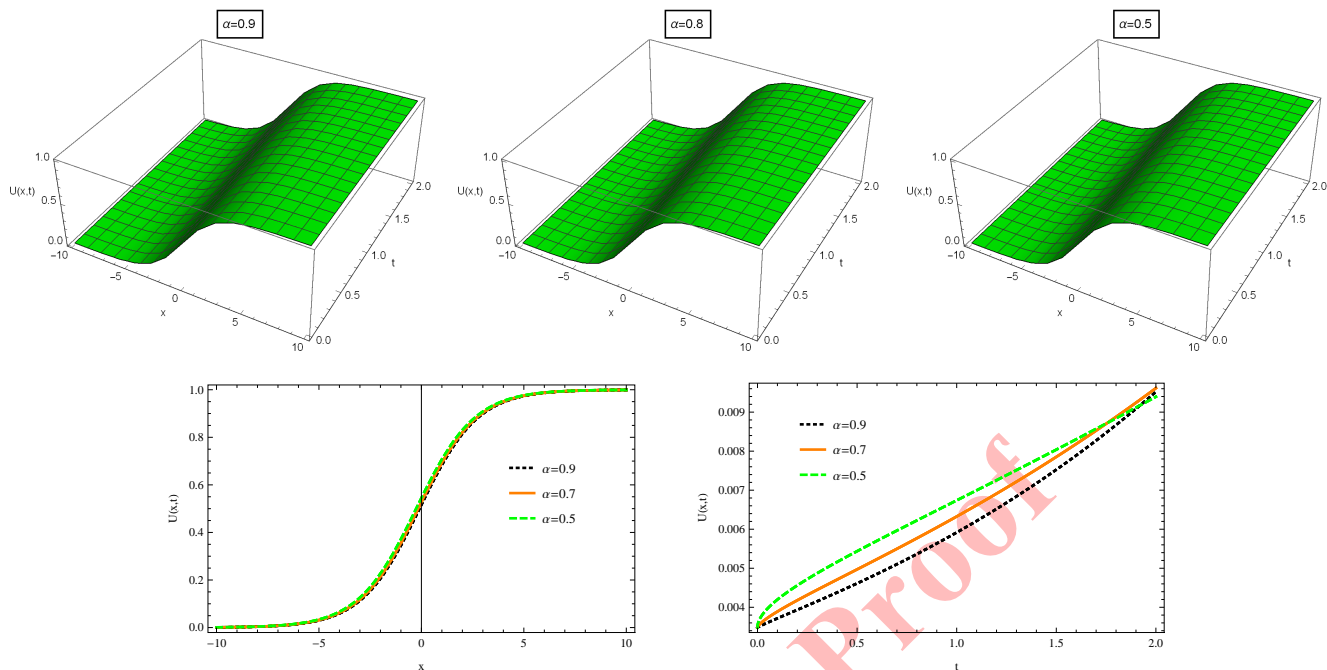


FIGURE 6. The behavior of approximate solution for $\mathcal{U}(x, t)$ problem 4.3 at $\alpha = 0.9, 0.8, 0.5$ in three dimensions as well as two dimensions with x at $t = 0.5$ and with t at $x = 5$.

TABLE 6. The exact solution, the approximate solution of MGMLFM (current results) for problem 4.3 and a comparison of the absolute error with MTST [13] at distinct values of x when $\alpha = 1, t = 0.1$ and $t = 0.5$.

x	$t = 0.1$				$t = 0.5$			
	Exact	MGMLFM	MGMLFM Error	MTST Error	Exact	MGMLFM	MGMLFM Error	MTST Error
-10	0.000892	0.000892075	1.75552×10^{-14}	4.16868×10^{-9}	0.001089	0.00108937	2.81931×10^{-10}	2.77828×10^{-7}
-8	0.003659	0.00365917	5.98467×10^{-14}	6.66744×10^{-8}	0.004465	0.0044657	9.54777×10^{-10}	2.79701×10^{-6}
-6	0.014881	0.0148815	6.73871×10^{-14}	1.05031×10^{-6}	0.018116	0.0181167	9.84808×10^{-10}	3.69676×10^{-5}
-4	0.058501	0.0585011	1.19446×10^{-12}	1.39130×10^{-5}	0.070530	0.0705398	1.95568×10^{-8}	4.44201×10^{-4}
6	0.986516	0.986516	6.95000×10^{-14}	3.25300×10^{-5}	0.988933	0.988933	1.13647×10^{-9}	8.04594×10^{-4}
8	0.996688	0.996688	5.91749×10^{-14}	8.52552×10^{-6}	0.997287	0.997287	9.05841×10^{-10}	2.12939×10^{-4}
10	0.999193	0.999193	1.75415×10^{-14}	2.11105×10^{-6}	0.999339	0.999339	2.63554×10^{-10}	5.28587×10^{-5}

TABLE 7. The exact solution, the approximate solution of MGMLFM (current results) for problem 4.3 and a comparison of the absolute error with HPM [13] at distinct values of x when $\alpha = 1, t = 0.2$ and $t = 0.8$.

x	$t = 0.2$				$t = 0.8$			
	Exact	MGMLFM	MGMLFM Error	HPM Error	Exact	MGMLFM	MGMLFM Error	HPM Error
-10	0.000937	0.00093777	1.75552×10^{-12}	1.44156×10^{-7}	0.001265	0.00126544	4.82935×10^{-9}	9.96713×10^{-6}
-8	0.003846	0.00384605	3.84983×10^{-12}	5.80186×10^{-7}	0.005184	0.00518464	1.62701×10^{-8}	4.00383×10^{-5}
-6	0.015632	0.0156326	4.24892×10^{-12}	2.18030×10^{-6}	0.020980	0.020987	1.55247×10^{-8}	1.49266×10^{-4}
-4	0.061316	0.0613166	7.73533×10^{-11}	6.07615×10^{-6}	0.081030	0.0810309	3.39545×10^{-7}	4.01265×10^{-4}
6	0.987165	0.987165	4.49618×10^{-12}	2.08616×10^{-6}	0.990460	0.99046	1.96338×10^{-8}	1.25134×10^{-4}
8	0.996849	0.996849	3.76943×10^{-12}	5.52665×10^{-7}	0.997664	0.997664	1.49582×10^{-8}	3.29636×10^{-5}
10	0.999232	0.999232	1.10112×10^{-12}	1.37172×10^{-7}	0.999431	0.999431	4.33561×10^{-9}	8.17059×10^{-5}



5. CONCLUSION

The FNM is considered one of the most crucial equations in the nerve impulse transmission process. The main objective of the current research is to investigate the solution of nonlinear FNM Eq. (1.4) and other special instances Eqs. (1.5) and (1.6) with the Caputo fractional operator. To achieve our goal, we successfully applied the MGMLFM to obtain the approximate solution for the time-fractional nonlinear FNM with initial values. The steps for solving general FPDEs using the suggested technique were demonstrated. Error analysis and MGMLFM convergence were also established for the obtained solutions. The theoretical results for the three proposed cases were supported by 2D and 3D graphics considering various fractional order α values. We contrasted the current findings for $\alpha = 1$ with the exact values. Additionally, we presented a numerical comparison between the estimated absolute error in the MGMLFM and other methods reported in the literature, including CSDM, HPM FRPS, and MTST. Based on our discussions, we found that the outcomes of the fractional nonlinear FNM employing MGMLFM are nearly identical to the exact solutions. Additionally, the absolute error estimated by MGMLFM is better compared to other published methods. The obtained results reinforce the plausibility and efficiency of the proposed method for examining different fractional-order nonlinear mathematical frameworks represented by FPDEs to describe a variety of real-world applications. The current work has very practical and intriguing implications, and it can assist upcoming researchers in analyzing the behavior of numerous nonlinear equations and models. Since the FNM is still open, future research will examine it further using improved schemes and an updated fractional operator.

REFERENCES

- [1] P. Agarwal, C. Cattani, and S. Momani, *Fractional Differential Equations: Theoretical Aspects and Applications*. Elsevier, 2024.
- [2] P. Agarwal, L. Vázquez, and E.K. Lenzi, *Recent trends in fractional calculus and its applications*. Recent Trends in Fractional Calculus and Its Applications, Elsevier, 1-290, 2024.
- [3] S. Alfaqeih, and E. Misirli, *On convergence analysis and analytical solutions of the conformable fractional Fitzhugh-Nagumo model using the conformable Sumudu decomposition method*. Symmetry, 13(2) (2021) 243.
- [4] H.M. Ali, *Analytical investigation of the fractional nonlinear shallow-water model*. J. Appl. Math. Comput., 2024 (2024) 1-18.
- [5] H. M. Ali, *An efficient approximate-analytical method to solve time-fractional KdV and KdVB equations*. Inf. Sci. Lett., 9(3) (2020) 189-198.
- [6] H. M. Ali, *New approximate solutions to fractional smoking model using the generalized Mittag-Leffler function method*. Progr. Fract. Differ. Appl., 5(4) (2019) 319-326.
- [7] H.M. Ali, K.S. Nisar, W.R. Alharbi, and M. Zakarya, *Efficient approximate analytical technique to solve nonlinear coupled Jaulent-Miodek system within a time-fractional order*. AIMS Mathematics, 9(3) (2024), 5671-5685.
- [8] M. Aychluh, D.L. Suthar, and S.D. Purohit, *Analysis of the nonlinear Fitzhugh-Nagumo equation and its derivative based on the Rabotnov fractional exponential function*. Partial Differ. Equ. Appl. Math., 11 (2024) 100764.
- [9] D. Baleanu, K. Diethelm, E. Scalas, and J. J. Trujillo, *Fractional Calculus: Models and Numerical Methods, Series on Complexity, Nonlinearity and Chaos*, Vol. 3, World Scientific Publishing Company, Singapore, New Jersey, London and Hong Kong, 2012.
- [10] D. Baleanu, and R.P. Agarwal, *Fractional calculus in the sky*. Adv. Diff. Eqs. 2021(1) (2021) 1-9.
- [11] A. Chakraborty, P. Veerasha, A. Cianciob, H. M. Baskonus, and M. Alsulami, *The effect of climate change on the dynamics of a modified surface energy balance-mass balance model of Cryosphere under the frame of a non-local operator*. Results Phys., 54 (2023) 107031.
- [12] A. Chakraborty, and P. Veerasha, *Effects of global warming, time delay and chaos control on the dynamics of a chaotic atmospheric propagation model within the frame of Caputo fractional operator*. Commun Nonlinear Sci Numer Simul., 128 (2024), 107657.
- [13] Z.Y. Fan, K. K. Ali, M. Maneea, M. Inc, and S.W. Yao, *Solution of time fractional Fitzhugh-Nagumo equation using semi analytical techniques*. Res. Phys., 51 (2023), 106679.
- [14] R. Fitzhugh, *Mathematical models of threshold phenomena in the nerve membrane*. Bull. Math. Biophys., 17 (1955), 257-269.



- [15] R. Fitzhugh, *Impulse and physiological states in models of nerve membrane*. Biophys J., 1 (1961), 445-466.
- [16] D. Fugarov, A. Dengaev, I. Drozdov, V. Shishulin, and A. Ostrovskaya, *Application of $\tan(\frac{\phi}{2})$ -expansion method for solving the fractional Biswas-Milovic equation for Kerr law nonlinearity*. Comput. Methods Differ. Equ., 2024 (2024), 1-19.
- [17] A. Ghorbani, *Beyond Adomian polynomials: He polynomials*. Chaos. Soliton. Fract., 39 (2009), 1486-1492.
- [18] W. Hamali, J. Manafian, M. Lakestani, A.M. Mahnashi, and A. Bekir, *Optical solitons of M-fractional nonlinear Schrdingers complex hyperbolic model by generalized Kudryashov method*. Opt. Quant Electron, 56 (2024), 7.
- [19] A.L. Hodgkin, and A.F. Huxley, *A quantitative description of membrane current and its application to conduction and excitation in nerve*. J. Physiol., 117 (1952), 500-505.
- [20] A.A. Kilbas, H.M. Srivastava, and J.J. Trujillo, *Theory and Applications of Fractional Differential Equations*. Elsevier, Amsterdam, 2006.
- [21] M. Lakestani, and J. Manafian, *Analytical treatments of the spacetime fractional coupled nonlinear Schrödinger equations*. Opt. Quant Electron, 50 (2018), 396.
- [22] J. G. Liu, and X. J. Yang, *Symmetry group analysis of several coupled fractional partial differential equations*. Chaos Solitons Fract., 173 (2023), 113603.
- [23] R. L. Magin, *Fractional Calculus in Bioengineering*. Volume 2, Begell House Redding, 2006.
- [24] J. Manafian Heris, and M. Lakestani, *Exact Solutions for the Integrable Sixth Order Drinfeld-Sokolov-Satsuma-Hirota System by the Analytical Methods*. Int. Sch. Res. Notices., 2014(1) (2014), 840689.
- [25] J. Manafian, M. Lakestani, and A. Bekir, *Comparison between the generalized tanh-coth and the $(\frac{G'}{G})$ -expansion methods for solving NPDEs and NODEs*. Pramana - J. Phys., 87 (2016), 95.
- [26] S. T. Mohyud-Din, M. A. Noor, and K. I. Noor, *Traveling wave solutions of seventh-order generalized KdV equations using he's polynomials*. Int. J. Nonlin Sci. Num., 10 (2009), 227-233.
- [27] J. Nagumo, S. Arimoto, and S. Yoshizawa, *An active pulse transmission line simulating nerve axon*. Proc IRE., 50 (1962) 2061-2070.
- [28] K. Pavani, and K. Raghavendar, *A novel method to study time fractional coupled systems of shallow water equations arising in ocean engineering*. AIMS Mathematics, 9(1) (2024), 542-564.
- [29] I. Podlubny, *Fractional Differential Equations, Mathematics in Sciences and Engineering*. Academic Press, San Diego, 1999.
- [30] A. Prakash, and H. Kaur, *A reliable numerical algorithm for a fractional model of Fitzhugh-Nagumo equation arising in the transmission of nerve impulses*. Nonlinear Engineering, 8(1) (2019), 719-727.
- [31] M. Shih, E. Momoniat, and F. M. Mahomed, *Approximate conditional symmetries and approximate solutions of the perturbed Fitzhugh-Nagumo equation*. J. Math. Phys., 46 (2005), 1-11.
- [32] S.A.Tarate, A.P. Bhadane, S.B. Gaikwad, and K.A. Kshirsagar, *Semi-analytical solutions for time-fractional cauchy reaction-diffusion equations via new Elazki transform iterative method*. Comput. Methods Differ. Equ., 2024 (2024), 1-16.
- [33] H. Thabet, S. Kendre, and J. Peters, *Travelling wave solutions for fractional Korteweg-de Vries equations via an approximate-analytical method*. AIMS Mathematics, 4(4) (2019), 1203-1222.

